

# ZnSe/GaAs(001) heterostructures with defected interfaces: structural, thermodynamic and electronic properties

A. Stroppa<sup>1, 2, \*</sup> and M. Peressi<sup>1, 2, †</sup>

<sup>1</sup>*Dipartimento di Fisica Teorica, Università di Trieste,  
Strada Costiera 11, I-34014 Trieste, Italy*

<sup>2</sup>*INFN DEMOCRITOS National Simulation Center, Trieste, Italy*

(Dated: December 2, 2024)

## Abstract

We have performed accurate *ab initio* pseudopotential calculations for the structural and electronic properties of ZnSe/GaAs(001) heterostructures with interface configurations accounting for charge neutrality prescriptions. Beside the simplest configurations with atomic interdiffusion we consider also some configurations characterized by As depletion and cation vacancies, motivated by the recent successfull growth of ZnSe/GaAs pseudomorphic structures with minimum stacking fault density characterized by the presence of a defected (Zn,Ga)Se alloy in the interface region. We find that—under particular thermodynamic conditions—some defected configurations are favoured with respect to undefected ones with simple anion or cation mixing, and that the calculated band offsets for some defected structures are compatible with those measured. Although it is not possible to extract indications about the precise interface composition and vacancy concentration, our results support the experimental indication of (Zn,Ga)Se defected compounds in high-quality ZnSe/GaAs(001) heterojunctions with low native stacking fault density. The range of measured band offset suggests that different atoms at interfaces rearrange, with possible presence of vacancies, in such a way that not only local charges but also ionic dipoles are vanishing.

PACS numbers: PACS: 73.40.Kp, 73.20.-r, 68.35.-p

## I. INTRODUCTION

II-VI/III-V heterostructures, whose prototype is ZnSe/GaAs, fabricated by molecular beam epitaxy (MBE) are important for electronic devices such as blue-green emitters<sup>1</sup> in optoelectronics, spin-transistors<sup>2,3</sup> and spin filters<sup>4</sup> in spintronics. For all the proposed applications, it is crucial to have a control of the structural quality of these interfaces and, in particular, of the native stacking fault (SF) defect density which causes serious device degradation.

The SFs density in II-VI/III-V interface is determined by the growth conditions. It has been suggested that the reduction of stacking fault density in the ZnSe/GaAs heterostructure can be achieved by inserting a thin low-temperature-grown ZnSe buffer layer between the high-temperature-grown ZnSe epilayer and the GaAs substrate, thus obtaining SF density as low as  $\sim 5.4 \times 10^4 \text{ cm}^{-2}$ <sup>5</sup>. More recently, two procedures have been found to work in reducing the SF density even below  $10^4 \text{ cm}^{-2}$  (thus providing a very high quality system), yielding quantitatively similar defected densities and qualitatively similar interface compositions and band alignments<sup>6</sup>.

A part from this experimental evidence, the microscopic mechanisms that control the native defect density in II-VI/III-V structures remain still controversial. What is noteworthy is that from an accurate characterization of the samples with minimum stacking fault density<sup>6</sup> there is experimental evidence of the formation of a ternary (Zn,Ga)Se alloy of variable composition with a substantial concentration of cation vacancies.<sup>7</sup> Because of vacancies, its average lattice parameter is smaller than the one of GaAs and ZnSe, and therefore this alloy is under tensile biaxial strain when epitaxially grown on GaAs substrates, accumulating a non negligible elastic energy. Evidence of formation of ordered binary defected compounds such as Ga<sub>2</sub>Se<sub>3</sub> or interface layers with vacancies arranged with other symmetry at ZnSe/GaAs interfaces has also been reported.<sup>8,9</sup> The defected compound Ga<sub>2</sub>Se<sub>3</sub> has also intentionally been grown epitaxially on GaAs<sup>10</sup> and, very recently, on Si(001) substrates<sup>11</sup> for its utilization in optoelectronics.

The driving mechanism for the formation of this defected alloy at ZnSe/GaAs interfaces is still unknown and, moreover, it is not clear whether defected interfaces could be favourite with respect to the simplest cases of cation and/or anion mixed interfaces without vacancies.

To this aim we have performed a comparative study based on *ab-initio* local-density-

functional pseudopotential approach of ZnSe/GaAs (001) heterostructures, including a few selected interface configurations with cation vacancies. Since charged interfaces are energetically unstable with respect to the interdiffusion of atoms across the interface<sup>12,13,14,15,16,17</sup> we consider interfaces satisfying the charge neutrality condition. Our comparative study will address their structural and electronic properties as well as their formation energy. This work is organized as follows: in the next section we describe the theoretical and computational approach; in Sect. III we describe the selected interface morphologies; in Sect. IV and V we report our results for the structural properties and relative stability; Sect. VI is devoted to the discussion of the electronic properties in terms of Density of States (Sect. VI-A) and band alignments (Sect. VI-B); finally, in Sect. VII we draw our conclusions.

## II. THEORETICAL AND COMPUTATIONAL METHOD

Our calculations are performed within the density functional theory framework using the local density approximation for the exchange-correlation functional<sup>18,19</sup> with state-of-the-art first-principles pseudopotential self-consistent calculations.<sup>20</sup> The wave functions are expanded onto a plane-wave basis set with a kinetic energy cutoff of 20 Ry: we carefully check that all the relevant bulk properties of the binary ZnSe and GaAs compounds are well converged. The Zn-3d electrons are taken into account only via the nonlinear core correction which has been shown to give reliable results for ZnSe, as discussed in Ref. 17. The integration over the Brillouin zone is performed using the special  $\mathbf{k}$ -point technique with a (6,6,6) Monkhorst-Pack mesh for the FCC cell and corresponding meshes for the various supercells.

The theoretical lattice constant of GaAs (ZnSe) is 1.8 % (1.4 %) smaller than the experimental lattice constant  $a_{exp}^{GaAs}=5.65$  Å<sup>21</sup> ( $a_{exp}^{ZnSe}=5.67$  Å<sup>21</sup>) but the small relative lattice mismatch is well reproduced ( $\leq 0.8$  %). In our calculations, we neglect this tiny lattice mismatch and we fixed the in-plane lattice constant to the theoretical one of GaAs which is typically the substrate in experimental samples. The ionic degrees of freedom are fully taken into account by optimizing the atomic positions via a total-energy and atomic-force minimization<sup>22</sup> with a threshold of 1 mRy a.u.<sup>-1</sup> for atomic forces and of 0.01 mRy for total energy changes between two consecutive relaxation steps.

The interfaces are modeled by tetragonal supercells with periodic boundary conditions

and contain a slab for each constituent material. We study the relative stability by considering the interface formation energy:<sup>23</sup>

$$2E_f^{intf} = \frac{(E_{supercell} - \sum_{i=1}^{N_{species}} n^i \mu^i)}{mn} \quad (1)$$

where  $E_{supercell}$  is the calculated total energy of the supercell,  $N_{species}$  is the number of the chemical species involved (which are 4 in the present case),  $n^i$  the number of atoms of the species  $i$  and  $\mu^i$  is the corresponding chemical potential;  $(m \times n)$  is the reconstruction (the in-plane periodicity of the interface), so that  $N = mn$  is the number of atoms in the two-dimensional interface unit cell and  $E_f^{intf}$  refers to a  $(1 \times 1)$  interface area. In general  $E_f^{intf}$  refers to a *mean* value of the formation energy of the two possibly inequivalent interfaces present in each supercell. We calculated the bulk chemical potentials considering the elemental forms of Zn (hcp),<sup>24</sup> Se (trigonal),<sup>24</sup> Ga (orthorhombic),<sup>24</sup> As (trigonal),<sup>24</sup> GaAs and ZnSe (cubic).<sup>21</sup> We employed the Gaussian smearing technique<sup>25</sup> for Brillouin integration of metallic systems. For each bulk elemental form we have chosen the proper  $k$ -point mesh which gives well converged values of the corresponding chemical potential, with a numerical uncertainty less than  $\approx 20$  meV per bulk formula units. The calculated heat of formation of bulk ZnSe and GaAs are  $-1.61$  eV and  $-0.80$  eV respectively which well compare with the experimental values ( $-1.67$  eV and  $-0.84$  eV):<sup>21,26</sup> this indirectly tests the reliability of our calculated elemental chemical potentials. They also agree with previous theoretical calculations.<sup>17,27,28,29,30</sup>

### III. INTERFACE STRUCTURES

We discuss in this Section the selected interface morphologies that we use as simplest models to describe the defected ZnSe/GaAs (001) junctions. Based on experimental suggestions about the formation of (Zn,Ga)Se compound in a As-depleted region<sup>7</sup> and for the sake of simplicity we consider only cation vacancies and we exclude the possibility of other defects such as interstitials or antisites.

For comparison, we preliminary consider the simplest interface morphologies with atomic intermixing limited to one or two atomic planes, without vacancies and satisfying the charge neutrality, already addressed in Refs. 15,17. The composition profiles for these simple cases are:

1C: 1-plane Cation-mixed:  $\cdots -\text{Ga-As-(Ga}_{\frac{1}{2}}\text{ Zn}_{\frac{1}{2}}\text{)-Se-Zn-}\cdots$

1A: 1-plane Anion-mixed:  $\cdots -\text{As-Ga-(As}_{\frac{1}{2}}\text{ Se}_{\frac{1}{2}}\text{)-Zn-Se-}\cdots$

2CA-ZnAs: 2-planes Cation-Anion mixed, Zn and As rich:  $\cdots -\text{As-Ga-(Se}_{\frac{1}{4}}\text{ As}_{\frac{3}{4}}\text{)-(Zn}_{\frac{3}{4}}\text{ Ga}_{\frac{1}{4}}\text{)-Se-Zn-}\cdots$

2CA-GaSe: 2-planes Cation-Anion mixed, Ga and Se rich:  $\cdots -\text{Ga-As-(Zn}_{\frac{1}{4}}\text{ Ga}_{\frac{3}{4}}\text{)-(Se}_{\frac{3}{4}}\text{ As}_{\frac{1}{4}}\text{)-Zn-Se-}\cdots$

The latter interfaces have no ionic dipole, as it would be the case for the abrupt, non-polar (110) interface. The interfaces 1C, 1A and 2CA-ZnAs, 2CA-GaSe are related by a simultaneous exchange of Ga with As and Zn with Se.

Introducing cation vacancies, many other different morphologies compatible with the charge neutrality condition are possible. We generalize the case of 1-plane Cation-mixed interface by considering the possibility of another Cation-mixed plane with vacancies as follows:



where V indicate vacancies and  $x, y, w, z$  are the in-plane atomic concentrations of the corresponding atomic species. The charge neutrality condition applied to this composition profile gives:

$$6(x + w) + 4(y + z) = 9 \quad (2)$$

$$x + y \leq 1 \text{ and } w + z \leq 1 \quad (3)$$

We note that Eq. 2 is symmetric under the exchange of  $x \leftrightarrow w$  and/or  $y \leftrightarrow z$ . In the following we focus only on the pairs of *complementary* solutions related by *both*  $x \leftrightarrow w$  and  $y \leftrightarrow z$  exchange and satisfy Eq.3: this corresponds to a *swap* of the cation planes across the Se plane.

First, we are going to consider systems with a high (H) local concentration of vacancies: in particular an interface plane with 50% concentration of vacancies, a configuration not very realistic but that can be easily simulated with small supercells. This case corresponds to  $x = \frac{1}{2}$ ,  $w = 1$ ,  $y = z = 0$  and the complementary solution, with the following composition profiles:

$1HV$ :  $\cdots - Ga - As - Ga_{\frac{1}{2}} - Se - Ga - Se - Zn - \cdots$

$1HV\text{-swap}$ :  $\cdots - Ga - As - Ga - Se - Ga_{\frac{1}{2}} - Se - Zn - \cdots$

These profiles are schematically shown in Fig. 1 together with a sketch of the bare ionic charge profile, averaged over two consecutive atomic planes and normalized to a bulk zincblende cell, indicating the extension and the value of the interface dipole.

Next, we consider the solutions with  $z=1$  and  $w=0$  which reduce to the case of vacancies just confined in a single plane between GaAs and ZnSe. Out of the possible cases, we select the one with  $x = \frac{5}{6}$  and  $y = 0$ . Considering also the swap across the Se plane, we have the following composition profiles:

$1V$ :  $\cdots - Ga - As - Ga_{\frac{5}{6}} - Se - Zn - Se - Zn - \cdots$

$1V\text{-swap}$ :  $\cdots - Ga - As - Zn - Se - Ga_{\frac{5}{6}} - Se - Zn - \cdots$

In terms of ionic charges, each Zn is equivalent to  $\frac{2}{3}$  of Ga, so that if we substitute Zn with  $Ga_{\frac{2}{3}}$  in the composition profiles of the possible neutral interfaces we still maintain the charge neutrality condition and we have:

$2V$ :  $\cdots - Ga - As - Ga_{\frac{5}{6}} - Se - Ga_{\frac{2}{3}} - Se - Zn - \cdots$  obtained from  $1V$ ;

$2V\text{-swap}$ :  $\cdots - Ga - As - Ga_{\frac{2}{3}} - Se - Ga_{\frac{5}{6}} - Se - Zn - \cdots$  obtained from  $1V\text{-swap}$ .

These interfaces have two planes with vacancies and correspond to  $x = \frac{5}{6}$ ,  $w = \frac{2}{3}$ ,  $y = z = 0$  and the complementary case  $x = \frac{2}{3}$ ,  $w = \frac{5}{6}$ ,  $y = z = 0$ .

All the interfaces considered above are characterized by the presence of Ga-Se and/or Zn-As bonds, which are not present in the bulk constituents. In general, at interfaces between heterovalent constituents there are “wrong” chemical bonds<sup>31</sup> with either more (“donor bond”) or less (“acceptor bond”) than two electrons. The charge neutrality rule can be equivalently expressed in terms of *compensation* of donor and acceptor bonds through reconstruction and atomic intermixing. Considering that recent experimental results do not indicate the presence of Zn-As bonds<sup>7</sup> we focus here mainly on structures with Ga-Se bonds and we include for comparison only one with Zn-As bonds, namely the one labelled as “ $1V\text{-swap}$ ”. Remarkably, in the entire range of the chemical potentials involved, the interface having Zn-As bonds is thermodynamically unstable with respect to the complementary one ( $1V$ ) which has the same stoichiometry but no Zn-As bonds (see Section V).

## IV. STRUCTURAL PROPERTIES

Because of the cation vacancies, lattice distortions are sizeable and affect mainly the anion sublattice. Below, we briefly discuss the structural properties of the different configurations studied. Lattice distortions have non negligible effects on electronic properties and stability of the system, which will be discussed in the next Section.

### A. Interfaces with 50% vacancies layer

Both 1HV and 1HV-swap supercells are characterized by a huge local concentration of cation vacancies, having a plane with 50% of vacancies. The supercells considered have 2 atoms per layer and 20 atomic layers (the total length of the supercell is 33.27 Å). Atomic relaxations are important in the interface region, and result in sizeable variations of the bond lengths—involving in particular of acceptor and donor bonds—and interplanar distances along the growth direction, which are reported in Fig. 2.

### B. Interfaces with different vacancy concentration

The supercell describing the 1(2)V and 1(2)V-swap interfaces have 6 atoms per layer and 20 atomic layers, with a total length of the supercells of 27.72 Å. In Fig. 2 we show the average interplanar distances along the [001] direction. In this cases, we have a non negligible buckling of the atomic planes, in particular in the interface region, which reduces progressively far from the interface, although propagating also several atomic layers far away, much more in 2V and 2V-swap than in 1V and 1V-swap. In Fig. 2 we report the average interplanar distances with an error bar determined by the maximum and minimum interlayer distances between adjacent atomic layers.

Although the composition profile along the growth direction is symmetric with respect to a middle plane in the constituent slabs, the two interfaces in the simulation cell are not equivalent in their 3D structure, and this justifies the lack of symmetry in the pattern of the interatomic distances. Incidentally, we note that the larger is the buckling in the interface region, the stronger is the effect propagating in the bulk slabs.

## V. THERMODYNAMIC STABILITY OF INTERFACES

We study the relative stability of the interfaces using Eq. (1). Although the precise values of the chemical potentials are unknown, strongly depending on the growth process and on the local environment, their range of variation and mutual relationships can be established in condition of thermodynamic equilibrium. In particular:

$$\mu_{GaAs}^{bulk} = \mu_{Ga} + \mu_{As} \text{ and } \mu_{ZnSe}^{bulk} = \mu_{Zn} + \mu_{Se} \quad (4)$$

for the equilibrium between the interface and the bulks;

$$\mu_i \leq \mu_i^{bulk} \quad (5)$$

to exclude the formation of precipitates (since when  $\mu_i = \mu_i^{bulk}$  the gas phase condensates to form the elemental bulk phase).

By defining the heat of formation of AB compound as:  $\Delta H_{AB} = \mu_{AB}^{bulk} - \mu_A^{bulk} - \mu_B^{bulk}$ ,<sup>17</sup> so that a negative  $\Delta H_{AB}$  means exothermic reaction, one gets the following relations:

$$\Delta H_{GaAs} + \mu_{As}^{bulk} \leq \mu_{As} \leq \mu_{As}^{bulk} \quad (6)$$

and

$$\Delta H_{ZnSe} + \mu_{Se}^{bulk} \leq \mu_{Se} \leq \mu_{Se}^{bulk}. \quad (7)$$

We choose  $\mu_{Zn} - \mu_{Ga}$  and  $\mu_{Se}$  as basic variables, and with some algebra we obtain:

$$\mu_{Zn}^{bulk} - \mu_{Ga}^{bulk} + \Delta H_{ZnSe} \leq \mu_{Zn} - \mu_{Ga} \leq \mu_{Zn}^{bulk} - \mu_{Ga}^{bulk} - \Delta H_{GaAs} \quad (8)$$

We can introduce new variables

$$\tilde{\mu}_{Zn} - \tilde{\mu}_{Ga} = \mu_{Zn} - \mu_{Ga} - (\mu_{Zn}^{bulk} - \mu_{Ga}^{bulk}) \quad (9)$$

and

$$\tilde{\mu}_{Se} = \mu_{Se} - \mu_{Se}^{bulk} \quad (10)$$

and discuss the relative stability of the interfaces in the ranges of variations of these variables.

We can specify Eq. (1) as follows:

$$2E_f^{intf} = \frac{E_{supercell} - N_{Se}\mu_{ZnSe}^{bulk} - N_{As}\mu_{GaAs}^{bulk} + (N_{Se} - N_{Zn})\mu_{Zn} + (N_{As} - N_{Ga})\mu_{Ga}}{mn} \quad (11)$$

The supercells with no vacancies that we have considered here are stoichiometric ( $N_{Se} = N_{Zn} = N_{ZnSe}$ , and  $N_{Ga} = N_{As} = N_{GaAs}$ ), therefore their formation energy is independent on the chemical potentials and Eq. (11) reduces to a constant value. The resulting interface formation energies for 1C and 1A are nearly degenerate, within 10 meV per  $(1 \times 1)$  interface unit cell. The same holds for 2CA-ZnAs and 2CA-GaSe. The relaxations lower the formation energies by 60 meV (50 meV) per interface unit cell for 1C and 1A, whereas the effect is stronger for 2CA-ZnAs and 2CA-GaSe where the formation energy is lowered by  $\sim 120$  meV per  $(1 \times 1)$  interface unit cell.

For the other structures, from Eq. (11) we obtain:

$$E_{f,1HV}^{intf} = C_{1HV} + (\tilde{\mu}_{Zn} - \tilde{\mu}_{Ga}) - \frac{1}{2}\tilde{\mu}_{Se} \quad (12)$$

$$E_{f,1V}^{intf} = C_{1V} + \frac{1}{3}(\tilde{\mu}_{Zn} - \tilde{\mu}_{Ga}) - \frac{1}{6}\tilde{\mu}_{Se} \quad (13)$$

$$E_{f,2V}^{intf} = C_{2V} + (\tilde{\mu}_{Zn} - \tilde{\mu}_{Ga}) - \frac{1}{2}\tilde{\mu}_{Se} \quad (14)$$

We observe that structures related by a swap of atomic planes have the same  $N_i$ 's, so they have the same expressions for the interface formation energy: therefore Eqs. (12,13, 14) also hold for the complementary structures. The constants  $C_i$  are characteristic of the specific interface and do not depend on the length of the supercell used: test calculations show that they change only by  $\sim 10$  meV per  $(1 \times 1)$  interface unit cell when increasing the length of the supercells: this is a further indication that the size of our supercells is large enough.

As it can be seen from Eqs. (12, 13,14), the interface energy  $E_f^{intf}$  is a linear function of  $\tilde{\mu}_{Zn} - \tilde{\mu}_{Ga}$  and  $\tilde{\mu}_{Se}$  with coefficients determined by the particular stoichiometry. It is convenient to discuss the dependence of  $E_f^{intf}$  on an individual variable separately, setting the other one equal to its limiting value given by Eqs. (7,8). In Fig. 3, we show the interface formation energies as a function of  $\tilde{\mu}_{Zn} - \tilde{\mu}_{Ga}$  for lower (upper) limit of  $\tilde{\mu}_{Se}$  (top) and as a function of  $\tilde{\mu}_{Se}$  for lower (upper) limit of  $\tilde{\mu}_{Zn} - \tilde{\mu}_{Ga}$  (bottom). The horizontal line corresponds to interfaces with no vacancies, namely 1C, 1A, 2CA-ZnAs, 2CA-GaSe which appear degenerate on the scale used. Right (left) hatched areas represent the range of variation of formation energy for 1HV, 1HV-swap, 2V, 2V-swap (1V, 1V-swap) configurations. The lowest formation energy for right (left) hatched area corresponds to 1HV (1V) configuration.

Now we discuss the limiting cases corresponding to  $\tilde{\mu}_{Se} = \Delta H_{ZnSe}$  and  $\tilde{\mu}_{Se} = 0$ , i.e. the lowest and uppermost values of  $\tilde{\mu}_{Se}$  (see Fig. 3, top part). The heat of formation for ZnSe

determines the lower limit of  $\tilde{\mu}_{Se}$  (see Eqs. 7,10).  $E_f^{intf}$  is a function of the other chemical potential. It can be seen that the most stable structures remain the same (1HV and the mixed ones with no vacancies) independently on the value of  $\tilde{\mu}_{Se}$ , although the value of  $(\tilde{\mu}_{Zn} - \tilde{\mu}_{Ga})$  at which they have competing energies changes a little bit. As a general trend, high values of  $\tilde{\mu}_{Se}$  should stabilize the formation of defected interfaces (in Fig. 3, top part, compare the  $\text{Max}\{\tilde{\mu}_{Se}\}$  respect to  $\text{Min}\{\tilde{\mu}_{Se}\}$  case). This observation agrees with previous calculation dealing with GaAs(001) surfaces where it has been shown that for an increasing Se chemical potential (high limit of  $\tilde{\mu}_{Se}$ ) the formation of a Ga vacancy beneath the surface becomes energetically favourable, driving the surface stoichiometry towards  $\text{Ga}_2\text{Se}_3$ .<sup>32</sup> On the other hand, substantial changes occur considering the extreme cases for  $\tilde{\mu}_{Zn} - \tilde{\mu}_{Ga}$  (see Fig. 3, bottom part). This indicates that the variation of  $\tilde{\mu}_{Se}$  has much less effect than a variation of  $\tilde{\mu}_{Zn} - \tilde{\mu}_{Ga}$ . This can be also argued from the different relative weight of the basic variables in Eqs. 12, 13, 14.

In the high  $\tilde{\mu}_{Se}$  limit (see Fig. 3, top part), the defected interfaces are favored over the mixed ones for almost the whole range of variation of  $\tilde{\mu}_{Zn} - \tilde{\mu}_{Ga}$ . At variance, in the limit of high  $\tilde{\mu}_{Zn} - \tilde{\mu}_{Ga}$  (see Fig. 3, bottom part) all the defected interfaces turn out to be unstable over the undefected mixed-ones, irrespectively on the variation of  $\tilde{\mu}_{Se}$ ; in the limit of low  $\tilde{\mu}_{Zn} - \tilde{\mu}_{Ga}$ , most defected interfaces are favored over the mixed-ones. Therefore a low  $\tilde{\mu}_{Zn} - \tilde{\mu}_{Ga}$  growth condition should favour the formation of defected interfaces.

For comparison with experiments, we observe that ZnSe is usually grown over a GaAs buffer, in a MBE chamber. Therefore the physically independent variables are  $\mu_{Zn}$  and  $\mu_{Se}$ . As far as  $\mu_{Se}$  is concerned, the uppermost value corresponds to Se-rich condition: in case of evaporation in UHV, like in the MBE chamber, this would be achieved with a low Zn/Se beam pressure ratio and consequently a high Se flux, with possible formation of cluster with a bulk-like crystal structure from the Se atoms deposited on surface. The physical interpretation of the other variable,  $\mu_{Zn} - \mu_{Ga}$ , is less straightforward. Moreover, in a MBE chamber,  $\mu_{Ga}$  can be considered as a constant as only Zn and Se atoms come from the effusion cells. Therefore the uppermost value of  $\mu_{Zn} - \mu_{Ga}$  should correspond to *rich* Zn condition (and viceversa). This interpretation is consistent with the above discussion about the dependence of formation energy on the basic variables. We also point out that, in principle, a different choice of basic variables is possible but this would not have affected the main results. Our choice is the simplest one.

We observe that 2V, 2V-swap, 1HV, 1HV-swap configurations have the same linear dependence on  $\tilde{\mu}_{Zn} - \tilde{\mu}_{Ga}$  and  $\tilde{\mu}_{Se}$  so that we can easily compare their relative stability in the whole range of variability of thermodynamic variables. Their relative order, from the most stable, is: 1HV, 2V, 2V-swap, 1HV-swap. If we define an average number of "wrong bonds" (including the *fictitious* bonds defined with the vacancies) per anion in the supercell, we can empirically observe that (at least for the relative stability among these structures) the most stable interface is the one with the lowest number of Se-Ga and As-V bonds and the highest number of Se-V bonds. On the other hand, 1V and 1V-swap are stoichiometric but differ for the presence of Zn-As bonds in the latter. As mentioned before, the 1V-swap configuration is unstable with respect to 1V, in the whole range of chemical potentials. This result is consistent with the experimental indication of Ga-Se bonds but no Zn-As bonds and with the results of Ref. 33 which is however limited to undefected interfaces and does not take into account the charge neutrality prescription.

Finally we caution the reader that we have just considered trends in relative stability among different interfaces only on the basis of thermodynamic arguments, and therefore the high relative stability of the interface with unrealistic concentration of vacancies has not an absolute validity. Kinetic effects should play an important role on stability and in particular could hinder the formation of interfaces with unrealistic vacancy concentration (see also discussion in Section VI B). Taking into account kinetic effects would go beyond the scope of the present study.

## VI. ELECTRONIC PROPERTIES

### A. Density of States

The presence of vacancies induces in general strong perturbations on the electronic states due to the large fluctuations of the crystalline field and may induce localized states at different energies. As an example, we report in Fig. 4 the total Density Of States (DOS) and the atomic Projected Density Of States (PDOS) on different atomic layers for the 1HV and 1HV-swap structures. In particular, the PDOS is shown from the topmost to the bottom panel for the sequence of atomic planes along the growth direction from the ZnSe side to the GaAs side through the plane with vacancies. It is also shown the "excess" DOS (black area),

defined as the difference between the PDOS and the corresponding bulk DOS, if positive. The vertical arrows in each panel denote the energy position of the cation and anion *s* states.

From the total DOS (topmost panels) it is evident that the main difference between the two structures with a high vacancy concentration in the interface region is the density of states in the forbidden energy gap: the structure 1HV is metallic, whereas the 1HV-swap structure maintains the semiconducting character of its constituents. Atomic relaxations tend to reduce the effects and to clean the gap, but not completely, as it can be seen comparing the two topmost panels for both 1HV and 1HV-swap structures (solid/dashed line for relaxed/unrelaxed structure)

Looking at the PDOS, it is clear that the gap states in the total DOS of the 1HV structure originate mainly from states localized in the interface region where the atomic species have "wrong" chemical bonds, with the major contribution deriving from the Ga layer sandwiched between two Se layers and to the Se atoms bonded to Ga atoms and vacancies. An effect of the strong local fluctuations of the crystalline potential in the interface regions is the variation in the energy position of the *s*-Se peaks with respect to their value in the bulk region and variation in the shape of the PDOS of Ga atoms bond to Se and As (see the arrows).

By inspection of the PDOS in the bulk sides we can see a large difference in the relative positions of the bulk *s*-Se and *s*-As peaks across the interface in the 1HV and 1HV-swap structures: in 1HV, the *s*-Se peaks are lower with respect to the *s*-As peaks by about 4 eV, whereas in the 1HV-swap structure this energy difference is strongly reduced and almost vanishing. This is related to the different ionic interface dipole due to the atoms swap, sketched in Fig. 1, and results also in different bands alignments, as discussed in the following Subsection.

Some of the effects of the fluctuations of the crystalline field can be explained with a simple model accounting for the "wrong" chemical bonds. We characterize these "wrong" bonds by defining the excess average ionic charge of the nearest-neighbors ( $NN$ ),  $\Delta z_{NN}$ ,<sup>34</sup> averaging also over the vacancies: if  $\Delta z_{NN}$  is positive (negative), the higher (lower) it is, the more (less) attractive it is the local potential with respect to a bulk environment.

In 1HV structure, the As atoms close to the plane of vacancies have  $\Delta z_{NN}=-0.75$ : they are in a crystalline potential less attractive than in the bulk and their valence band states are shifted upwards in the direction of the forbidden energy gap. The other atoms in the

interface region have a positive  $\Delta z_{NN}$ :  $\Delta z_{NN} = 0.5, 1.0, 0.25, 0.5$ , respectively, for the Se layer between Zn and Ga, for Ga between Se layers, for Se between Ga layers, and for the Ga plane with vacancies. A crystalline potential more attractive than the bulk one pushes down in energy the states from the conduction band. This roughly explains the origin of the gap states in this structure.

In the 1HV-swap structure, the local fluctuations of the crystalline field are weaker. Se atoms between the Zn and the  $\text{Ga}_{0.5}$  layer with vacancies show electronic states not very different with respect to the bulk; and Zn atoms nearest to the interface region (with  $\Delta z_{NN}=0$ ) also show features similar to the bulk. The Se atoms sandwiched between two Ga planes (with  $\Delta z_{NN}=0.25$ ), strongly differ from the bulk case but not in the region of the energy gap.

Extending our analysis to the other defected interfaces studied here, we notice that the presence of electronic states within the energy gap is a common feature, and the 1HV-swap structure is an exception.

## B. Band alignments

We summarize schematically in Fig. 5 the band alignments calculated for the selected structures considered here. We follow the approach of Ref. 35, splitting the band offset into two contributions:  $VBO = \Delta E_v + \Delta V$ , where  $\Delta E_v$  is the band structure term, i.e. the energy difference between the relevant valence band top edges of the two materials measured with respect to the average electrostatic potential in the corresponding bulk crystal and  $\Delta V$  is the electrostatic potential lineup containing all interface-specific effects and extracted from supercell calculations. The potential lineup in turn includes a contribution related to the ionic dipole and its screening (indicated as  $\Delta V_{hetero}$  in Ref. 35) plus a term which is purely electronic and independent on interface details. The spin orbit effects are added *a posteriori* using experimental data.

As predicted for the heterovalent heterostructures, the band alignments are strongly dependent on the specific interface morphology. This is particularly true in the occurrence of vacancies, as it can be easily seen by inspection of Fig. 5: for undefected (without vacancies) interfaces the maximum variation is of the order of 1 eV (compare 1C and 1A cases),<sup>15,36,37</sup> whereas it is much larger in case of vacancies by changing their concentration and position,

the extreme variation (of about 4 eV) being found for 1HV and 1HV-swap structures, where the alignment changes from the so-called “broken gap” type (1HV) to “staggered” (1HV-swap). We point out that such a huge variation is associated to unrealistically high local concentration of vacancies. In real samples we expect vacancies diluted over a larger interface region.

In the spirit of *linear response theory* (LRT)<sup>12,35,38</sup> the variation of band offset in heterovalent heterojunctions has been rationalized and quantitatively explained in terms of the line-ups associated to the different interface ionic charge distribution and the corresponding electronic screening, i.e. of  $\Delta V_{hetero}$ . Neglecting details such as optimized atomic positions, simple calculations based on elementary electrostatics and LRT give  $\Delta V_{hetero} = \pi e^2 / 2a_0 \langle \epsilon \rangle \approx 0.5$  eV for 1C, 1V and 2V, the opposite for 1A,  $\Delta V_{hetero} = 0$  for 2CA-ZnSe and 2CA-GaSe, and  $\Delta V_{hetero} = 9\pi e^2 / 2a_0 \langle \epsilon \rangle \approx 4$  eV for 1HV and  $\Delta V_{hetero} = -3\pi e^2 / 2a_0 \langle \epsilon \rangle \approx -0.33$  eV for 1HV-swap, where  $a_0$  is the lattice constant and  $\langle \epsilon \rangle$  a proper average<sup>39</sup> between the dielectric constant of GaAs and ZnSe (which are 10.86 and 5.7 for GaAs and ZnSe respectively<sup>40</sup>). By comparing the LRT predictions with the full self-consistent calculations reported in Fig. 5 we can comment about the validity of the LRT: its predictions are quantitatively correct for undefected structures, but fails with discrepancies up to 1 eV in case of vacancies (LRT predicts band offset 1V and 2V equal to 1C, and 1V-swap equal to 2V-swap). It is not surprising: the LRT better holds in case of interface configurations without vacancies since the perturbation due to the presence of the interface is related to rather small differences between atoms (e.g. Zn vs. Ga, Se vs. As), and it is expected to be less accurate in case of strong perturbations such as vacancies.

The measured variation of the band offset in real samples obtained with different growth procedures is much lower than what found here for different vacancy configurations: it is limited to about 0.6 eV, as indicated by the range of the experimental data in the right hand side of Fig. 5 with the label “Exp(2)”. We show separately the right hand side of Fig. 5 with the label “Exp(1)” the experimental values from Ref. 7, ranging from  $0.60 \pm 0.05$  eV to  $0.72 \pm 0.10$  eV for the two samples with lowest SF density, whose composition of the interface region is indicated to be 45 at% Se, 34 at% Zn, 21 at% Ga and 50 at% Se, 40 at% Zn, 10 at% Ga respectively. A common indication extracted from the experiments is a type-I or “straddling” band alignment (the band edges in the GaAs slab are both *within* the band gap of ZnSe): remarkably, this is qualitatively compatible with most configurations studied

here, including some with vacancies.

It is not possible to extract any precise indication on the morphology of real samples from the comparison between experimental results and numerical predictions: there are many different configurations which can give the same band offsets and, moreover, relative stability crucially depends of the kinetics of the growth process. However, we can conclude that the occurrence of vacancies is compatible with the experimentally measured band offsets, and the most likely configurations in real samples seems to be characterized not only by charge neutrality but also by vanishing ionic dipoles.

## VII. CONCLUSION

We have studied with accurate ab-initio calculations several selected interface configurations for the ZnSe/GaAs(001) heterojunctions satisfying the charge neutrality condition, including also defected configurations with cation vacancies. We have shown that in some particular thermodynamic conditions (basically *rich*-Se chemical potential) the formation of defected interfaces with cation vacancies is even favoured over the simpler, undefected, unstrained, anion- and/or cation-mixed interfaces. We would like to note that one of the procedure leading to interface with low SF's density (and vacancy at interface) involve fabrication of ZnSe buffer layer at interface in highly Se-rich condition.<sup>7</sup> The band alignments are strongly dependent on the particular interface morphology, in particular in the occurrence of vacancies; on the other hand, different morphologies can correspond to the same or to similar band offsets, so that a unique correspondence between morphology, band offset, relative thermodynamic stability cannot be established. Nevertheless, the predicted stability of some defected interfaces and the compatibility of predicted band alignments with measurements support the experimental evidence of (Zn,Ga)Se defected compounds in high-quality ZnSe/GaAs(001) heterojunctions with low native stacking fault density. The range of measured band offset suggests that different atoms at interfaces rearrange, with possible presence of vacancies, in such a way that not only local charges but also ionic dipoles are vanishing.

## VIII. ACKNOWLEDGMENTS

We gratefully acknowledge E. Carlino, A. Franciosi and A. Colli for fruitful discussions. Computational resources have been obtained partly within the “Iniziativa Trasversale di Calcolo Parallelo” of the Italian *Istituto Nazionale per la Fisica della Materia* (INFM) and partly within the agreement between the University of Trieste and the Consorzio Interuniversitario CINECA (Italy).

---

\* Electronic address: astroppa@ts.infn.it

† Electronic address: peressi@ts.infn.it

- <sup>1</sup> O. Schulz, M. Strassburg, T. Rissom, S. Rodt, L. Reissmann, U.W. Pohl, D. Bimberg, M. Klude, D. Hommel, S. Itoh, K. Nakano, *Phys. Stat. Sol. B* **229**, 943 (2002) and references therein.
- <sup>2</sup> I. Malajovich, J.J. Berry, N. Samarth and D.D. Awschalom, *Nature (London)* **411**, 770 (2001).
- <sup>3</sup> S.A. Wolf, D.D. Awschalom, R.A. Buhrman, J.M. Daughton, S. von Molnar, M.L. Roukes, A.Y. Chtchelkanova, D.M. Treger, *Science* **294**, 1488 (2001).
- <sup>4</sup> P. Grabs, G. Richter, R. Fiederling, C.R. Becker, W. Ossau, G. Schmidt, L.W. Molenkamp, W. Weigand, E. Umbach, I.V. Sedova, S.V. Ivanov, *Appl. Phys. Lett.* **80**, 3766 (2002) and references therein.
- <sup>5</sup> J.S. Song, D.C. Oh, H. Makino, T. Hanada, M.W. Cho, T. Yao, Y.-G. Park, D. Shindo, J.H. Chang, *J. Vac. Sci. Technol. B* **22**, 607 (2004)
- <sup>6</sup> A. Colli, E. Pelucchi, A. Franciosi, *Appl. Phys. Lett.* **83**, 81 (2003).
- <sup>7</sup> A. Colli, E. Carlino, E. Pelucchi, V. Grillo, and A. Franciosi, *J. Appl. Phys.* **96**, 2592 (2004).
- <sup>8</sup> D. Li, J.M. Gonsalves, N. Otsuka, J. Qiu, M. Kobayashi, R.L. Gunshor, *APL* **57**, 449 (1990)
- <sup>9</sup> T. Okamoto et al., in *Ternary and Multinary Compounds in the 21th century*, IPAP Book 1, p 162 (2001)
- <sup>10</sup> L.H. Kuo, K. Kimura, A. Ohtake, S. Miwa, T. Yasuda, T. Yao, *J. Vac. Sci. Technol. B* **15**, 1241 (1997).
- <sup>11</sup> T. Ohta, D.A. Schmidt, S. Meng, A. Klust, A. Bostwick, Q. Yu, M.A. Olmstead, F.S. Ohuchi, *Phys. Rev. Lett.* **94**, 116102 (2005).
- <sup>12</sup> W. A. Harrison, E. A. Kraut, J. R. Waldrop and R.W. Grant, *Phys. Rev B* **18**, 4402 (1978).

- <sup>13</sup> R.M. Martin, *J. Vac. Sci. Technol. B* **17**, 978 (1980).
- <sup>14</sup> G. Bratina, L. Vanzetti, L. Sorba, G. Biasiol, A. Franciosi, M. Peressi, S. Baroni, *Phys. Rev. B* **50**, 11723 (1994).
- <sup>15</sup> R. Nicolini, L. Vanzetti, G. Mula, G. Bratina, L. Sorba, A. Franciosi, M. Peressi, S. Baroni, R. Resta, A. Baldereschi, J.E. Angelo, and W.W. Gerberich, *Phys. Rev. Lett.* **72**, 294 (1994).
- <sup>16</sup> R.G. Dandrea, S. Froyen, and A. Zunger, *Phys. Rev. B* **42**, R3213 (1990).
- <sup>17</sup> A. Kley and J. Neugebauer, *Phys. Rev. B*, **50**, 8616 (1994).
- <sup>18</sup> D.M. Ceperley and B.J. Alder, *Phys. Rev. Lett.* **45**, 566 (1980).
- <sup>19</sup> J.P. Perdew and A. Zunger, *Phys. Rev. B* **23**, 5048 (1981).
- <sup>20</sup> S. Baroni, A. Dal Corso, S. de Gironcoli, and P. Giannozzi, <http://www.pwscf.org>
- <sup>21</sup> R. Blachnik and O. Madelung, in *Numerical data and Functional Relationships in Science and Technology*, edited by O. Madelung, M. Schulz, and H. Weiss, Landolt-Börnstein, New Series, Group X, Vol.17, Pt.a (Springer, New York, 1982); H.E. Gumlich, D. Theis, and D. Tschierse, *ibid.*, Pt. b.
- <sup>22</sup> For the optimization of atomic position we require Hellmann-Feynman forces smaller then 0.02 eV Å<sup>-1</sup>.
- <sup>23</sup> G.X. Qian, R.M. Martin, and D.J. Chadi, *Phys. Rev. B* **37**, 1303 (1988).
- <sup>24</sup> J. Donohue, *The structures of the elements* (New York, Wiley, 1974).
- <sup>25</sup> C. L. Fu and K. M. Ho, *Phys. Rev.* **28**, 5480 (1983)
- <sup>26</sup> F. Bechstedt and R. Enderlein, *Semiconductor Surfaces and Interfaces* (Berlin, Akademie Verlag, 1988).
- <sup>27</sup> L.G. Wang, A. Zunger, *Phys. Rev. B* **68**, 125211 (2003).
- <sup>28</sup> W.G. Schmidt and F. Bechstedt, *Phys. Rev. B* **54**, 16742 (1996).
- <sup>29</sup> G.-X. Qian, R.M. Martin, and D.J. Chadi, *Phys. Rev. Lett.* **60**, 1962 (1988).
- <sup>30</sup> T. Ohno, *Phys. Rev. Lett.* **70**, 631 (1993).
- <sup>31</sup> W.R.L. Lambrecht, C. Amador, and B. Segall, *Phys. Rev. Lett.* **68**, 1363 (1992).
- <sup>32</sup> S. Gundel, W. Spahn, W. Faschinger, G. Landwehr, *J. Cryst. Growth*, **184/185**, 80 (1998).
- <sup>33</sup> H.H. Farrel and Randall A. LaViolette, *J. Vac. Sci. Technol. B* **22**, 2250 (2004).
- <sup>34</sup> M. Peressi, F. Favot, G. Cangiani, and A. Baldereschi, *Appl. Phys. Lett.* **81**, 5171 (2002).
- <sup>35</sup> M. Peressi, N. Binggeli, and A. Baldereschi, *J. Phys. D* **31**, 1273 (1998).
- <sup>36</sup> S. Kumar, S.N. Jha, Jagannath, T. Ganuli, S.V.B. Bhaskara Rao, N.C. Das, *Appl. Surf. Science*,

**229**, 324 (2004).

<sup>37</sup> M. Funato, S. Aoki, S. Fujita, J. Appl. Phys. **85**, 1514 (1999).

<sup>38</sup> A. Franciosi and C.G. VandeWalle, Surf. Sci. Rep. **25**, 1 (1996).

<sup>39</sup> M. Peressi, L. Colombo, R. Resta, S. Baroni, and A. Baldereschi, Phys. Rev. B 48, 12 047 (1993).

<sup>40</sup> O. Madelung, in *Semiconductors: data handbook*, 3rd ed. ,Springer, Berlin, (2004).

FIG. 1: Composition and bare ionic charge profiles (in unit of electronic charge per zincblende unit cell) in the interface region of the defected heterostructures 1HV, 1HV-swap, 1V, 1V-swap, 2V, 2V-swap along the (001) growth direction. The ionic charge is averaged over pairs of adjacent (001) atomic layers and normalized to the bulk zincblende unit cell. Interface cationic planes are emphasized in boldface.

FIG. 2: Interplanar distances (in Å) for the different structures considered including cation vacancies. The average value of the interplanar distances are indicated by closed symbols, and the error bar indicate the range of local variation due to the possible buckling of the atomic planes.

FIG. 3: Top: Formation energy [in eV/1×1 surface] of the mixed and defected interfaces as a function of the difference of the Zn and Ga chemical potentials, for lower(upper) limit of  $\tilde{\mu}^{Se}$ . Dotted lines refer to the undefected 1C, 1A, 2CA-ZnAs, 2CA-GaSe interfaces, which appear degenerate on this energy scale. Hatched areas indicate the range of interface formation energy for interfaces with the same stoichiometry: right (left) hatched areas represent the range of variation of formation energy for 1HV, 1HV-swap, 2V, 2V-swap (1V, 1V-swap). Those with the lowest formation energy are 1HV-swap and 1V for the two families respectively. Bottom: as before, as a function of the difference of the Se chemical potential for the lower (upper) limit of  $\tilde{\mu}^{Zn} - \tilde{\mu}^{Ga}$ . The chemical potentials have been rescaled with respect to their correspondent bulk value (see text).

FIG. 4: Total DOS (upper panels) and atomic Projected Density of States over layers along the growth direction for the 1HV (panels a) and 1HV-swap (panels b) interface. The "excess" DOS is shown as black area (see text). Arrows indicate the energy position of the cation and anion *s* states in each layer. Energies are referred to the Fermi energy for 1HV and to the Valence Band Maximum for 1HV-swap. Solid/dashed line in the topmost panels are for relaxed/unrelaxed structure.

FIG. 5: Scheme of the band alignments for the different interfaces investigated. The relative energy scale is referred to the band edges of GaAs, which are indicated on the left, and the relative position of ZnSe is then indicated for the different morphologies. The horizontal dotted lines refer to GaAs band edges. The label “Exp(1)” refers to experimental values in Ref.7 and “Exp(2)” to all the other measurements reported in the literature<sup>15</sup>.

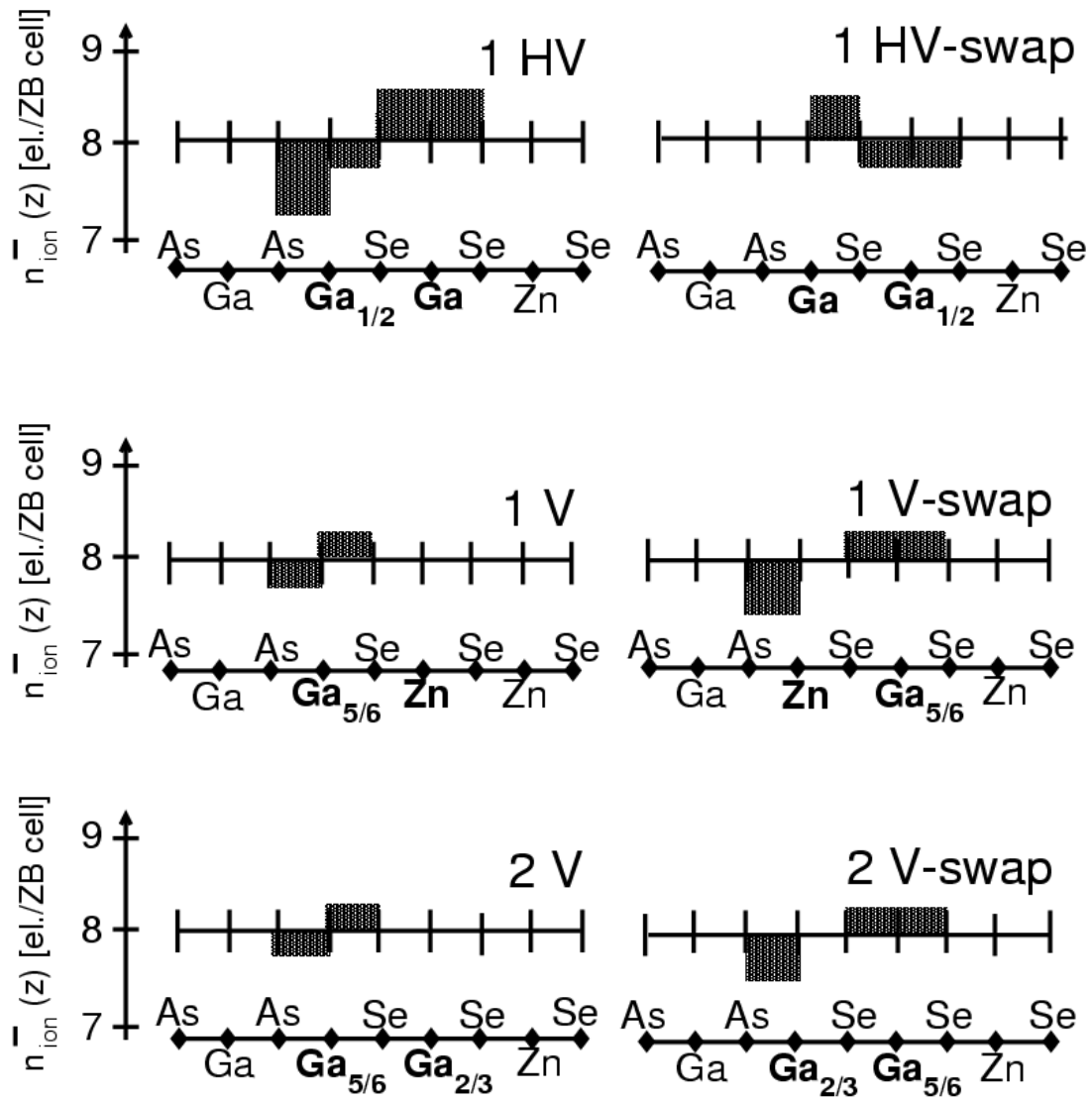


Fig. 1

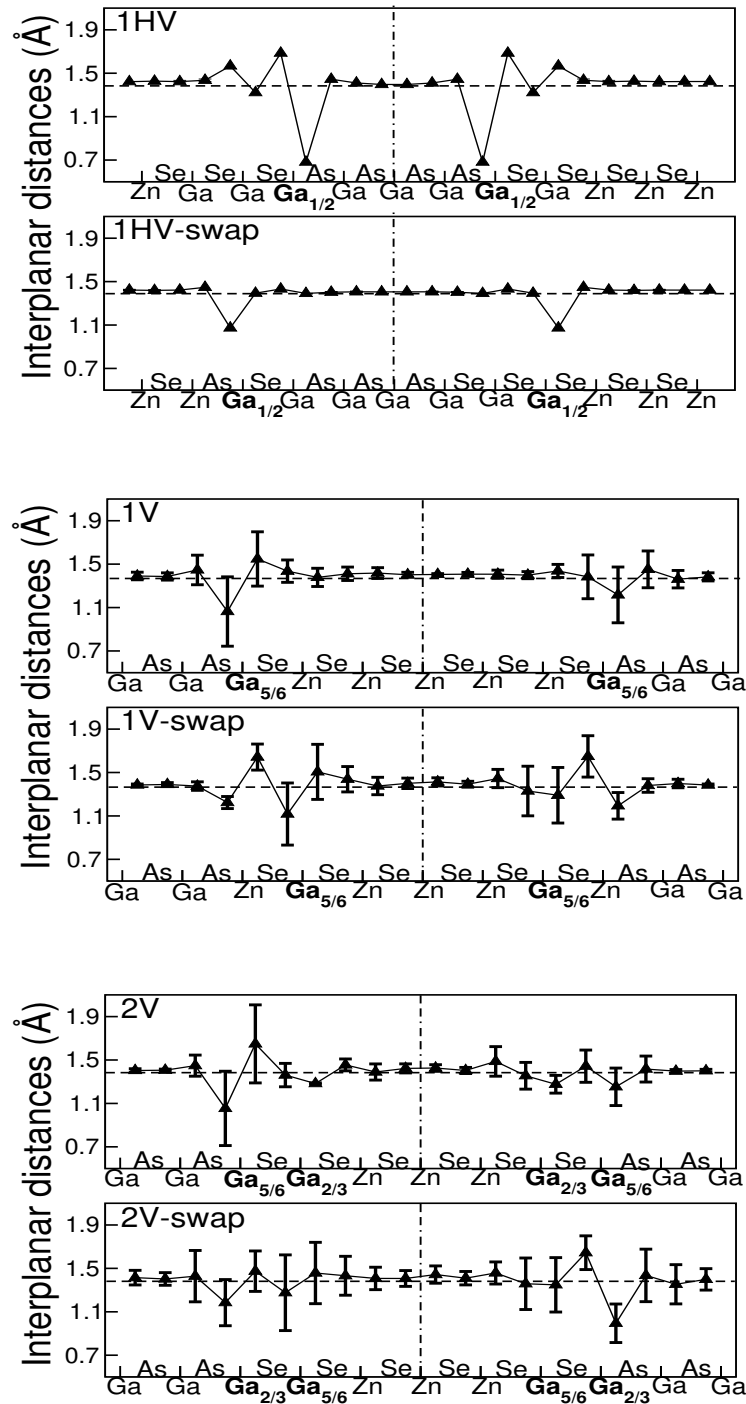
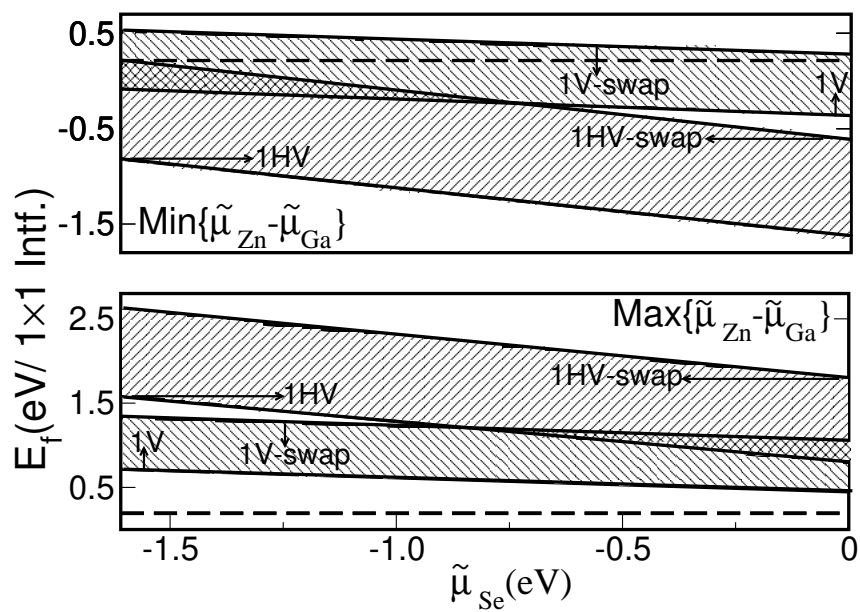
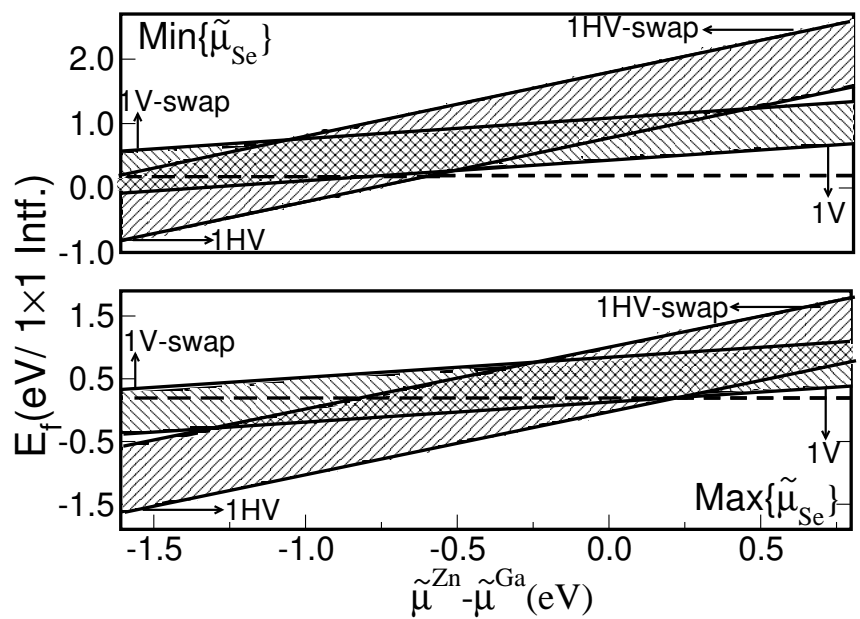


Fig. 2



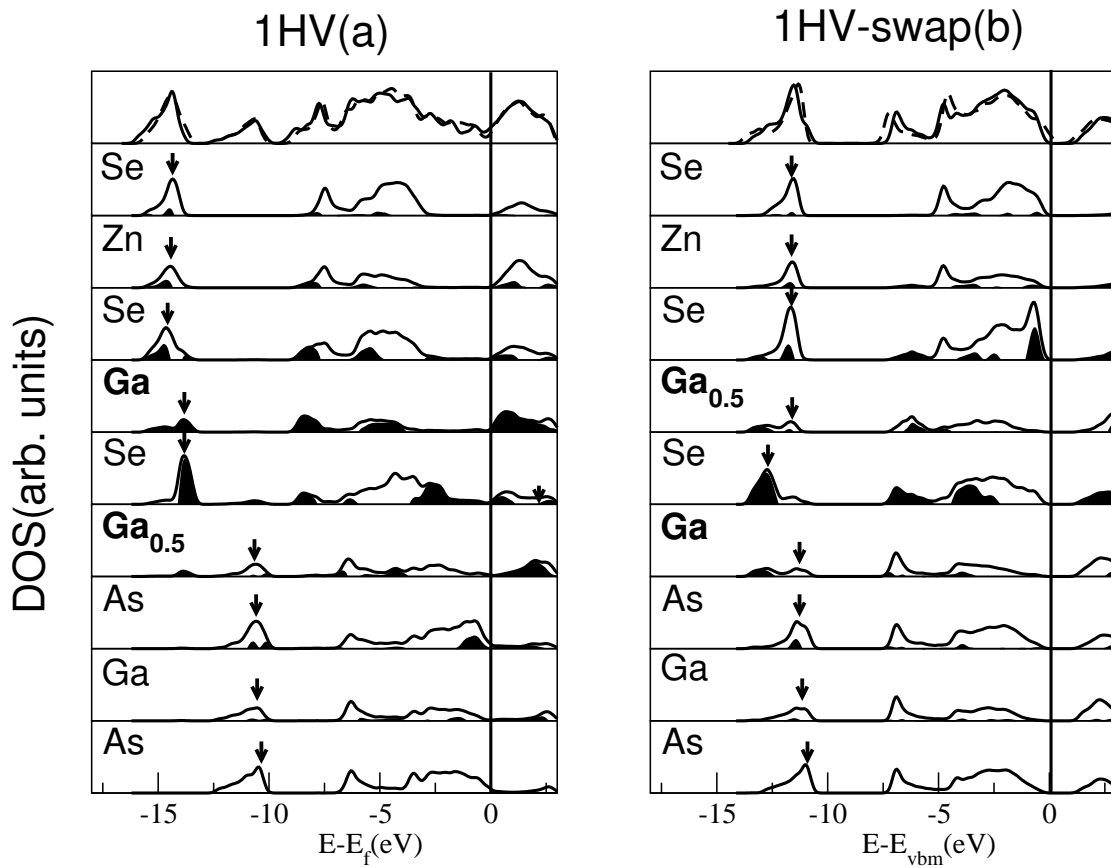


Fig. 4

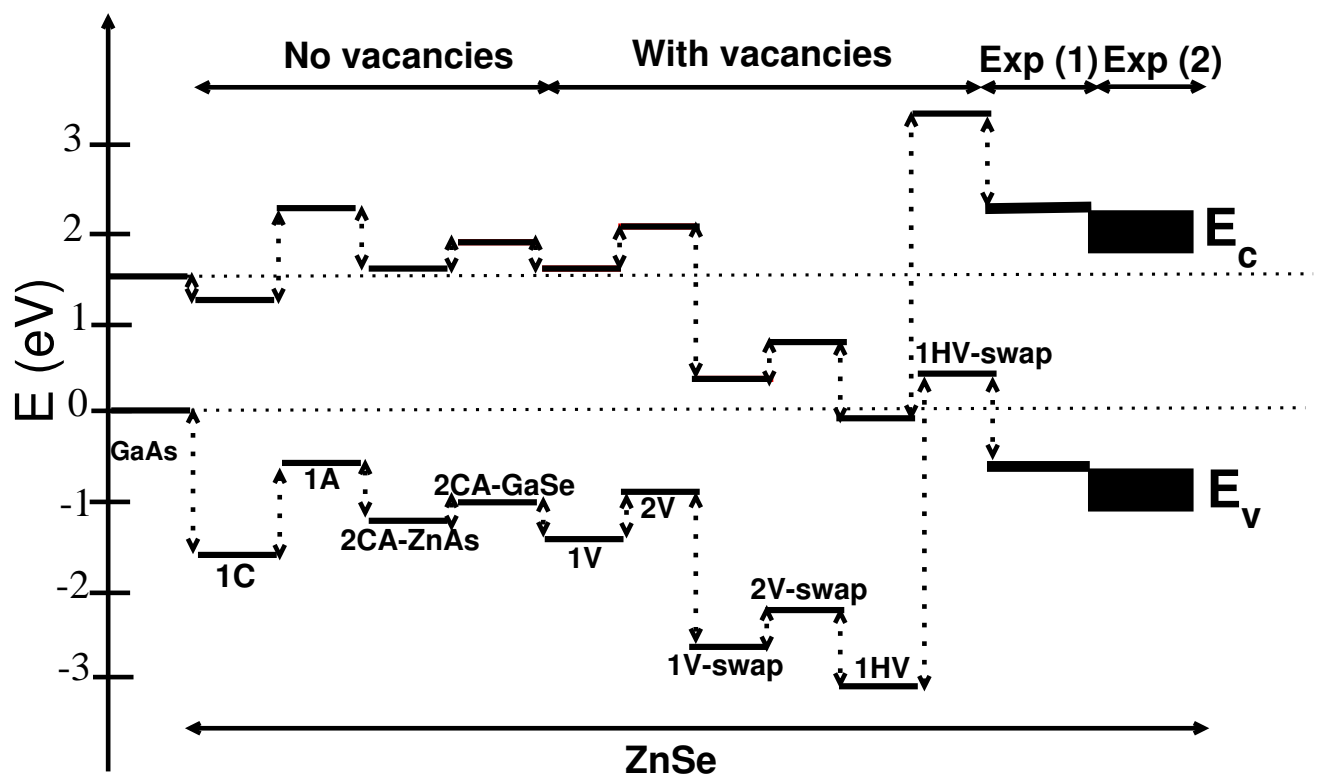


Fig. 5